Appendage regeneration requires IMPDH2 and creates a sensitized environment for enzyme filament formation

Morgan E. McCartney[1], Gavin M. Wheeler[1], Audrey G. O'Neill[1,2], Jeet H. Patel[3], Zoey R. Litt[1], S. John Calise[1], Justin M. Kollman[1], Andrea E. Wills[1]*

1. Department of Biochemistry. University of Washington, Seattle WA
2. Program in Biological Physics, Structure, and Design. University of Washington, Seattle WA
3. Department of Cell and Developmental Biology, University of Pennsylvania, Philadelphia PA
* *to whom correspondence should be addressed: aewills@uw.edu*

Summary

The regeneration of lost tissue requires biosynthesis of metabolites needed for cell proliferation and growth. Among these are the purine nucleotides ATP and GTP, which are required for diverse cellular processes including DNA synthesis, cytoskeletal assembly, and energy production. The abundance and balance of these purines is regulated by inosine monophosphate dehydrogenase 2 (IMPDH2), which catalyzes the committing step of GTP synthesis. IMPDH2 is typically expressed at high levels in proliferating cells and assembles into filaments that resist allosteric inhibition under conditions of high GTP demand. Here we asked whether IMPDH2 is required in the highly proliferative context of regeneration, and whether its assembly into filaments takes place in regenerating tissue. We find that inhibition of IMPDH2 leads to impaired tail regeneration and reduced cell proliferation in the tadpole *Xenopus tropicalis*. Upon treatment with IMPDH inhibitors, we find that both endogenous and fluorescent fusions of IMPDH2 robustly assemble into filaments throughout the tadpole tail, and that the regenerating tail creates a sensitized condition for filament formation. These findings clarify the role of purine biosynthesis in regeneration and reveal that IMPDH2 enzyme filament formation is a biologically relevant mechanism of regulation in vertebrate regeneration.

Keywords: Xenopus; regeneration; IMPDH2; purine; nucleotide metabolism; enzyme filament

Graphical Abstract

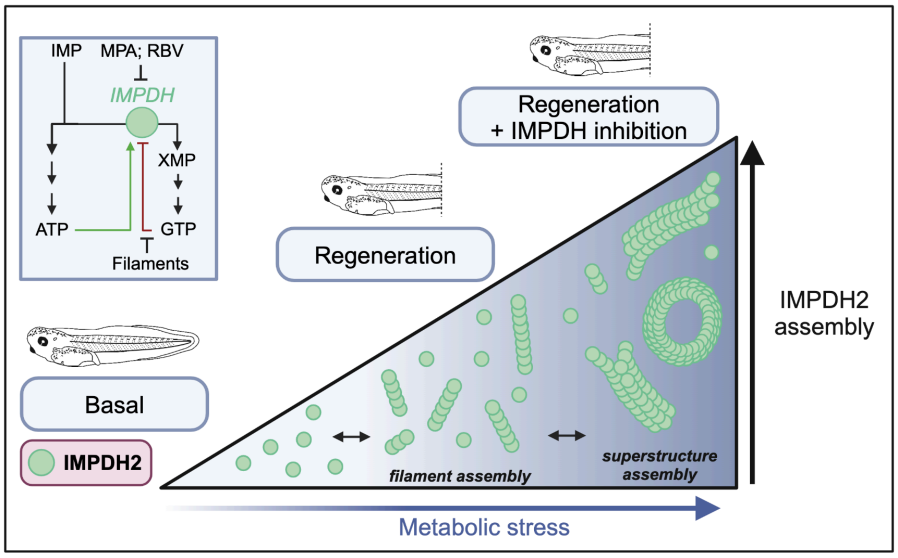

Results

Recently, we described an increased demand for glucose during *Xenopus* tail regeneration and a role for the pentose phosphate pathway (PPP) as a principal fate of that glucose, especially in proliferating cells.[1] The PPP yields several useful intermediates for biosynthesis, including ribulose-5-phosphate, a common precursor of nucleotide metabolism.[2] During cell proliferation, nucleotides are in high demand for DNA and RNA synthesis as well as cytoskeletal remodeling. Following up on those observations, we turned our attention here to the question of whether nucleotide biosynthesis is a limiting condition or under specific regulation during tail regeneration. Downstream of the PPP, the enzyme inosine monophosphate dehydrogenase (IMPDH) sits at a major regulatory node in *de novo* nucleotide biosynthesis by catalyzing the committing step in the production of guanine nucleotides rather than adenine nucleotides[3] (**Figure 1A**). Structurally, IMPDH constitutively forms tetramers that reversibly dimerize into either extended, active octamers in the presence of ATP or compressed, inactive octamers in the presence of GTP.[4] Under conditions of purine stress, such as IMPDH inhibition, octamers assemble into filaments that structurally resist GTP-induced octamer compression, sustaining enzyme activity in the presence of normally inhibitory levels of GTP.[4] Filaments can further assemble laterally to create filament superstructures that can be several microns long.[5–9] The role of IMPDH, and the physiological relevance of filament formation, has not been tested in a regenerative context.

IMPDH2 is required for cell proliferation and growth during tail regeneration

We hypothesized that IMPDH2, the isoform of IMPDH commonly expressed in proliferating cells[10–13], might play a specific role in regenerating tissues, where high purine demand relative to the rest of the tadpole would promote IMPDH2 filament assembly. To test this hypothesis, we investigated IMPDH2 expression, function, and filament formation during *Xenopus tropicalis* tail regeneration. To ask if IMPDH2 was required during regeneration, we amputated tadpole tails at 3 days post fertilization (Nieuwkoop and Faber stage 41), followed by treatment with the IMPDH2 inhibitor mycophenolic acid (MPA) (**Figure 1B**). MPA acts as an uncompetitive inhibitor of IMPDH2, binding in the NAD+ site.[14–17] As an alternative inhibitor, we also used Ribavirin (RBV), which when converted to Ribavirin 5'-monophosphate in the cell, acts as a competitive inhibitor and binds in the IMP site.[18] Uninjured tadpoles were tolerant of both MPA and RBV, showing neither morphological nor behavioral defects when treated with 200 µM MPA or 1 mM RBV at stage 41 (data not shown). Treatment during regeneration with either 100 µM MPA or 500 µM RBV resulted in significantly shorter regenerated tails at 72 hours post amputation (hpa)(Figure **1C-E, I**). While there are many cellular processes that depend on purine nucleotides, among those with the highest demand is cell proliferation. To divide, cells need ATP and GTP for DNA replication, actin and microtubule assembly, motor protein function, and energetic currency. It follows that cell division would likely be sensitive to perturbations of IMPDH2 during regeneration. Consistent with this prediction, we detected significantly decreased density of mitotic nuclei marked by phospho-histone H3 (pH3) in the regenerating tail of tadpoles treated with either MPA or RBV compared to untreated tadpoles (**Figure 1F-H, J**). These results show that inhibition of IMPDH2 impairs normal tail regeneration and limits cell proliferation in *Xenopus* tadpoles.

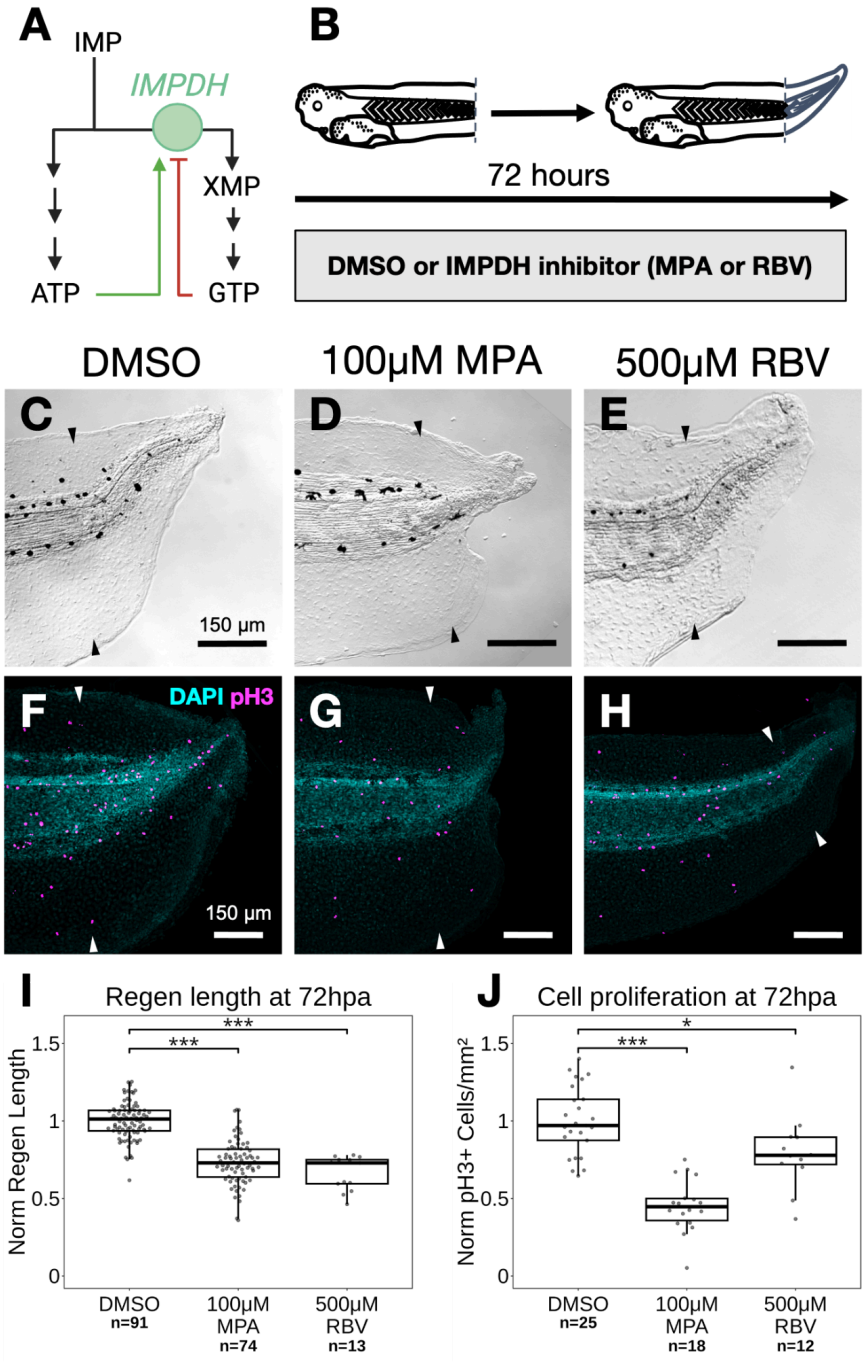

Figure 1. IMPDH inhibition impairs regeneration and cell proliferation.

(A) Simplified pathway diagram of IMPDH2 highlighting regulation by purine nucleotides.

(B) Schematic of experimental design. Tadpoles are amputated and then allowed to regenerate for 72 hours in media supplemented with either vehicle control (DMSO) or IMPDH inhibitor (MPA or RBV).

(C-E) DIC images of tadpole tails 72 hours post amputation (hpa) treated with either 0.05% DMSO, 100 μM MPA, or 500 μM RBV. Arrows indicate the plane of amputation.

(F-H) Immunohistochemistry (IHC) for proliferative marker pH3 at 72 hpa. Arrows indicate the plane of amputation.

(I-J) Quantification of regeneration defects following IMPDH inhibition. Regenerate length (I) and $pH3^{+}$ cell density in regenerating tissue (J) normalized to DMSO condition by experimental clutch at 72 hpa. Statistical significance between conditions was determined by ANOVA followed by Tukey's HSD test. *$p < 0.05$; *** $p < 0.001$.

IMPDH2 expression during tail regeneration

Because IMPDH2 was required for normal growth and cell proliferation during regeneration, we hypothesized that it might be strongly upregulated during regeneration to meet the increasing purine demand of cell proliferation. To test this, we examined expression of IMPDH2 and other purine biosynthesis enzymes during tail regeneration. First, we analyzed our previously published bulk RNA-Seq data[19] for expression of all the enzymes used in *de novo* purine biosynthesis. This dataset comprises all the cell types of the tail. We found that while most purine biosynthesis enzymes are significantly upregulated at 24 hpa, IMPDH2 itself is not significantly changed (**Figure 2A, B**). We then used *in situ* hybridization to examine IMPDH2 expression levels and localization. Prior to injury, IMPDH2 is generally expressed at lower levels in the tail tip than the remainder of the tail, but during regeneration, it is upregulated in the tail tip at 72 hpa relative to uninjured stage matched controls (**Figure 2C**). Expression of *impdh2* in the uninjured tail was largely localized to the somites, as has also been observed in zebrafish.[20] To query protein expression, we performed a western blot for IMPDH2 in regenerating or uninjured tadpole tails. We amputated tadpole tails and then collected tail tissue from either regenerating tadpoles or their stage matched uninjured counterparts at 0, 24, or 72 hpa. We find that IMPDH2 protein levels actually decrease markedly in both uninjured and regenerating tadpoles from stage 41 to stage 47, and are comparable in regenerating tails at 72 hpa relative to uninjured stage-matched tails (**Figure 2D, Supplemental Figure 1**). Thus, IMPDH2 transcript levels are unchanged early in regeneration, but appear to be specifically upregulated in regenerating tissues by 72 hpa. Protein levels, by contrast, are similar in regenerating versus uninjured stage-matched tissue at all stages.

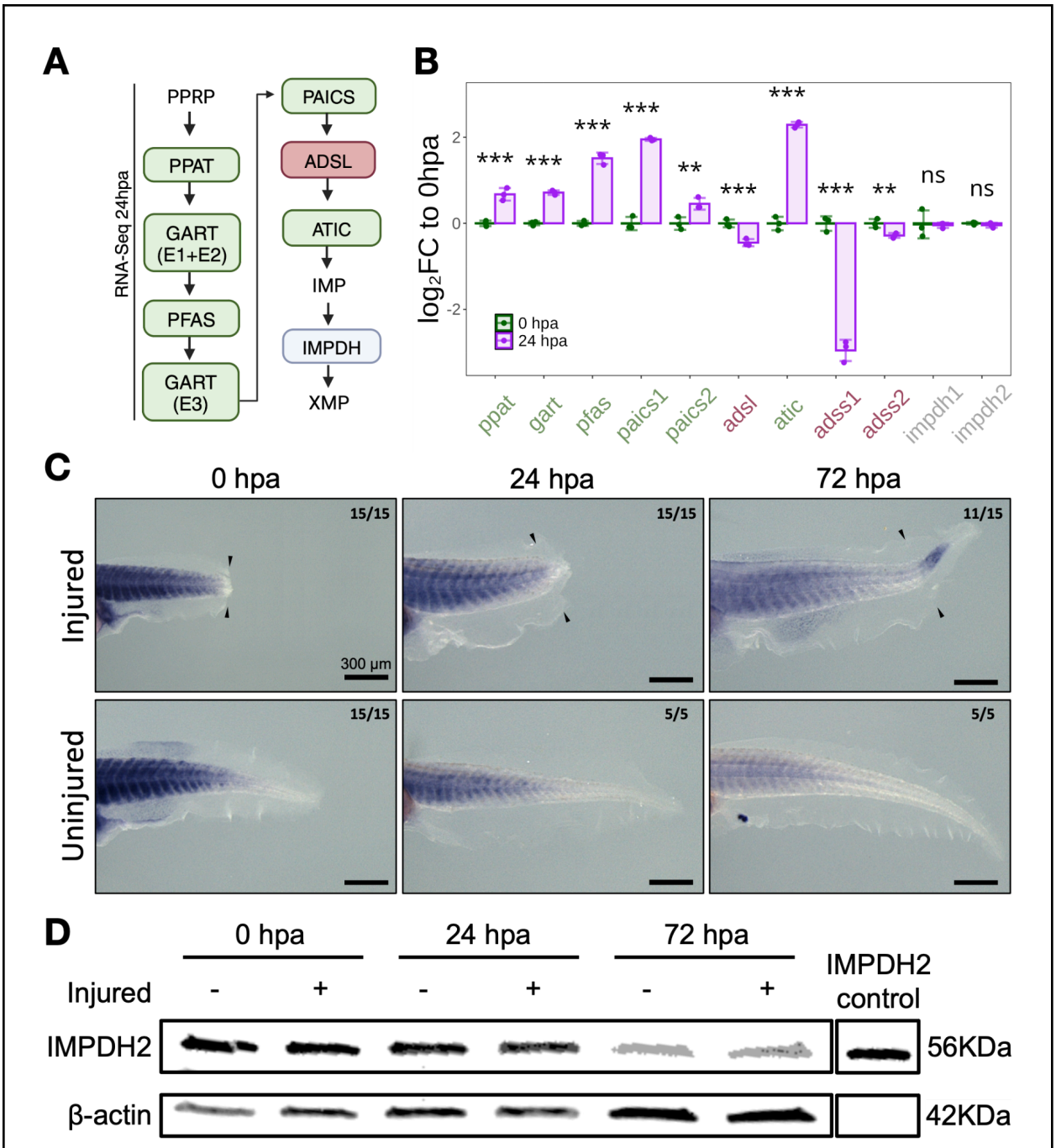

Figure 2. IMPDH2 expression during regeneration.

(A) Schematic of the *de novo* purine synthesis pathway upstream of IMPDH. Phosphoribosyl pyrophosphate (PRPP) enters and is converted into inosine monophosphate (IMP) before commitment by IMPDH into xanthine monophosphate (XMP) and ultimately GTP. Enzymes are boxed with fill color representing an overall increase (green) or decrease (red) in transcript levels at 24 hpa.

(B) Expression of *de novo* purine synthesis genes at 0 and 24 hpa as log_2FC to 0 hpa mean. Statistical significance was determined using EdgeR. **p < 0.01; ***p < 0.001; ns, not significant.

(C) *In situ* hybridization of *impdh2* at 0, 24, and 72 hpa in injured and uninjured tadpoles. Expression appears concentrated in muscle tissue, with somitic boundaries clearly visible. Overall expression declines during development, but increases specifically in the regenerating tissue at 72 hpa. Numbers in the top right of each panel indicate the number of samples that resemble the representative image over the total number assayed. Arrows indicate the plane of amputation.

(D) Western blot for IMPDH2 and β-actin in injured (+) or uninjured (-) tails at 0, 24, and 72 hpa.

IMPDH2 forms filaments in the tail following inhibition

The modest changes in IMPDH2 expression led us to wonder if other mechanisms of IMPDH2 regulation might contribute to its function during regeneration. Specifically, allosteric regulation by filament formation might be a different mode by which IMPDH2 activity is modulated in this context. IMPDH2 is allosterically regulated by GTP and ATP, and by assembly into filaments. IMPDH2 filaments reconstituted *in vitro* have been shown to structurally resist GTP-induced compression, decreasing sensitivity to feedback inhibition and allowing the enzyme to maintain activity. In cells, IMPDH2 filaments bundle together into filamentous superstructures under conditions of high GTP demand.[4] To examine the localization of endogenous IMPDH2, we performed immunofluorescence on uninjured tadpoles. IMPDH2 was diffuse throughout the tadpole tail under control conditions (**Figure 3A, B, E**), similar to IMPDH2 in untreated cells in culture. However, after treatment with MPA or RBV, filamentous superstructures formed throughout the tail (**MPA: Figure 3C, F; RBV: Figure 3D, G**). The superstructures appear identical to “rods and rings" described in cultured cells and typically measured between 2-10 μm in diameter or length. Superstructures assembled in most tail tissues, including fins, but were most abundant in axial tissues, where they were distributed in a segmental pattern that matched the periodicity of somites (**Figure 3C, D**). To observe superstructures in live tissue, we created an IMPDH2-RFP fusion construct. mRNA encoding this fusion protein was injected at the 2 cell stage. These embryos were reared to stage 41, at which point they were treated with MPA and live imaged (**Figure 3H**). We found that superstructures were detectable in injected tadpoles 24 hours after MPA treatment (**Figure 3I, J**), affirming that superstructures can form in live tissues and are not artifacts of fixation.

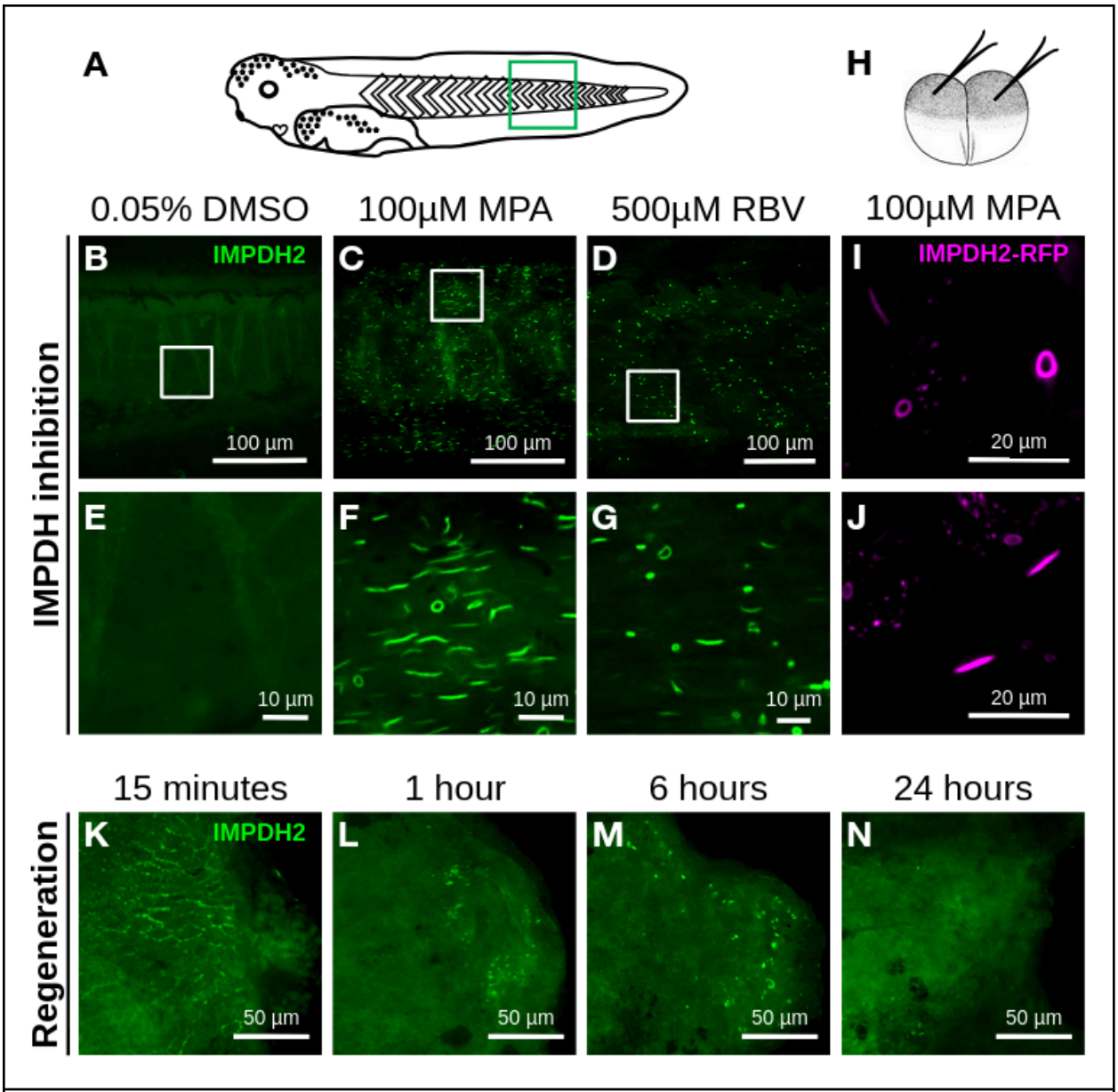

Figure 3. IMPDH2 forms filaments in the tail following inhibition.

(A) Tadpole diagram. Green box denotes approximate imaging location.

(B-D) Immunohistochemistry (IHC) for IMPDH2 in St. 47 tadpole tails after 72 hour treatment with 0.05% DMSO (B), 100 µM MPA (C), or 500 µM RBV (D). White boxes indicate location of close-up images shown in (E)-(G).

(E-G) Close-up images of panels (B), (C), and (D) respectively.

(H) mRNA microinjection diagram at the 2-cell stage. Embryos were injected with 1000 pg of mRNA encoding IMPDH2-RFP fusion protein.

(I-J) Images of live St. 45 tadpoles expressing IMPDH2-RFP fusion protein after 24 hour treatment with 100 μM MPA. IMPDH2-RFP forms both Ring Superstructures (I) and Rod Superstructures (J) in the tadpole tail under IMPDH2 inhibition.

(K-N) IHC for IMPDH2 during wound closure and early regeneration. Images were taken of the axial tissue at the amputation site.

(K) At 15 minutes post amputation, IMPDH2 appears localized to the membrane in epidermal cells proximal to the amputation site in 7/8 samples.

(L) By 1 hour small punctae begin to form near the injury in 6/7 samples.

(M) By 6 hours the small punctae appear to have assembled into slightly larger structures reminiscent of “rod and ring” superstructures in 9/10 samples.

(N) By 24 hours the signal around the wound site is once again diffuse and mostly free of any structures in 8/10 samples.

The regenerating tail creates a sensitized environment for IMPDH2 filament formation

We next hypothesized that regenerating tissues would have a greater purine demand than uninjured tissue, and thus be more likely to assemble IMPDH2 filaments into superstructures. To test this hypothesis, we first amputated tadpole tails and allowed them to regenerate for up to 72 hours in normal or control (DMSO) media, followed by fixation and staining for IMPDH2. We saw that shortly after amputation, IMPDH2 transiently localized to cell membranes and punctae near the amputation plane, suggesting rapid dynamics for IMPDH2 localization immediately after injury (**Figure 3K-N**). Filamentous structures were rarely observed in DMSO-treated regenerating tails at 72 hpa (**Figure 4A-D**). We next asked whether the regenerating tail might create a sensitized environment for superstructure formation. More specifically, we hypothesized that the threshold for forming superstructures in regenerating tissue would be lower than in uninjured tissue, requiring lower doses of inhibitor to induce them. Consistent with this hypothesis, we found that treatment with low doses of MPA (1-10 μM) produced very few superstructures in the anterior trunk far from the amputation plane (**Figure 4E, F, I, J**), but abundant superstructures in the newly regenerated tail tissue (**Figure 4G, H, K, L**). Whereas at higher doses of MPA (25 μM), superstructures formed in both the trunk and the regenerating tail tip (**Figure 4M-P**). The number of superstructures per unit area was higher in regenerating tissue at 1 μM and 10 μM MPA relative to non-regenerating trunk tissue (**Figure 4S**). A similar sensitization was seen for RBV, in which filaments were observed in regenerating tissue but not in non-regenerating tissue at 100 μM RBV (**Supplementary Figure 2**). This shows that regenerating tissue is sensitized to IMPDH2 inhibition, and closer to the threshold of purine stress required for filament formation relative to non-regenerating tissue.

Finally, to confirm that superstructures are formed in the sensitized condition due to purine depletion, rather than direct inhibition of IMPDH2, we asked whether superstructures

would form if the regenerating tissue was supplied an alternative source of GTP. To this end, we treated amputated tadpoles with a surplus of guanosine in addition to MPA. Guanosine is converted into guanine and subsequently GMP by the purine salvage pathway, bypassing IMPDH2 in the *de novo* synthesis pathway. We found that in the 1 µM MPA sensitized condition, supplementation with 200 µM guanosine was sufficient to reduce the assembly of superstructures to that of the control after 72 hours of regeneration (**Figure 4Q vs R, T**).

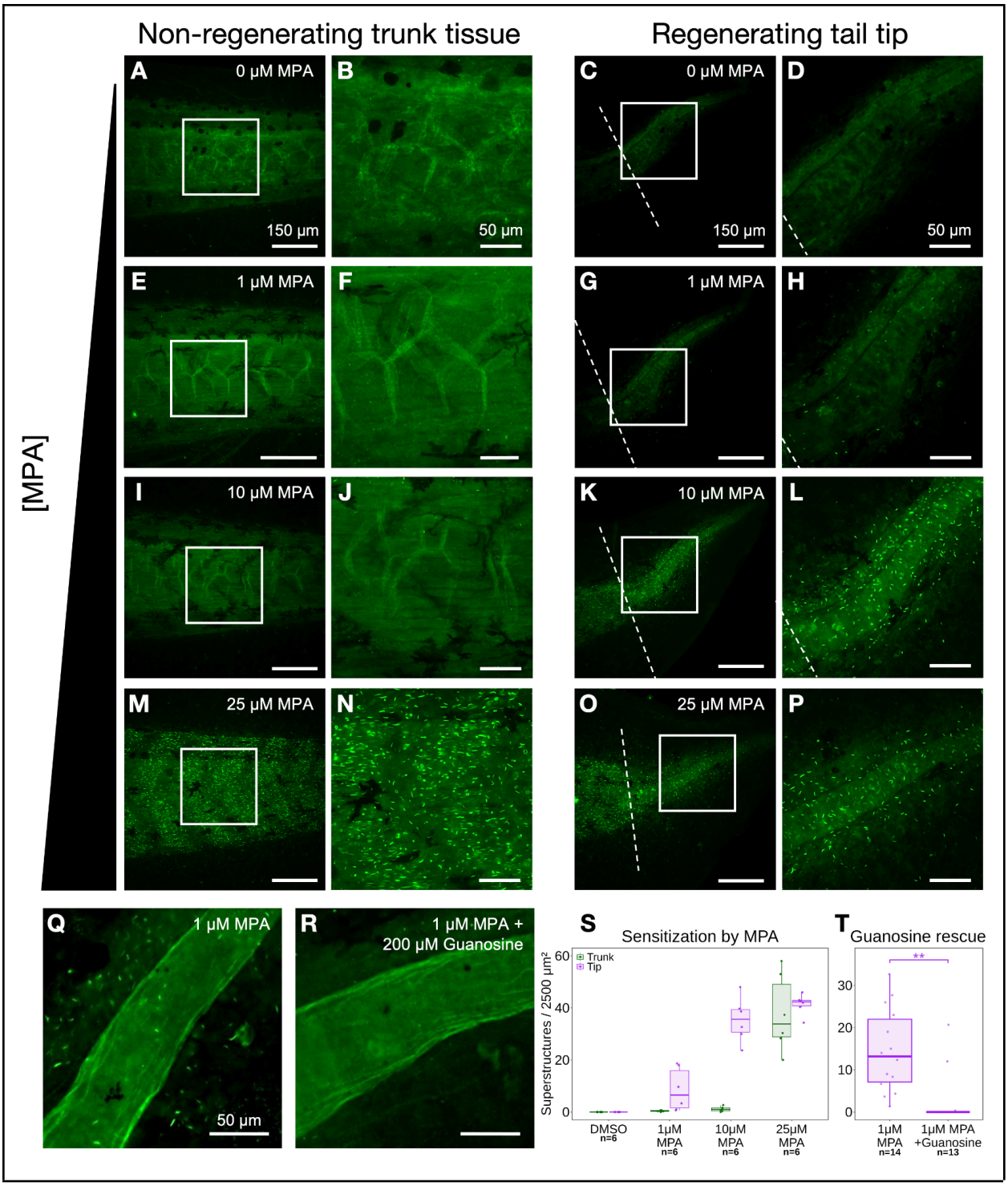

Figure 4. The regenerating tail creates a sensitized environment for IMPDH2 filament formation.

(A-D) IHC for IMPDH2 in 72 hpa tadpoles treated with 0.05% DMSO. IMPDH2 filaments rarely assemble under control conditions in the non-regenerating trunk tissue (A and B) or the regenerating tail tip (C and D).

(E-H) IHC for IMPDH2 in 72 hpa tadpoles treated with 1 μM MPA. IMPDH2 filaments do not assemble in the non-regenerating trunk tissue (E and F). Filaments do assemble in the regenerating tail tissue (G and H).

(I-L) IHC for IMPDH2 in 72 hpa tadpoles treated with 10 μM MPA. IMPDH2 forms few filaments in the non-regenerating trunk tissue (I and J). IMPDH2 filaments assemble robustly in the regenerating tail tip (K and L).

(M-P) IHC for IMPDH2 in 72 hpa tadpoles treated with 25 μM MPA. IMPDH2 filaments assemble robustly in the non-regenerating trunk tissue (M-N) and the regenerating tail tip (O-P).

(Q-R) IHC for IMPDH2 in 72 hpa tadpoles. IMPDH2 filaments form in the regenerating tail tip after treatment with 1 μM MPA (Q). Filament formation is reduced in the regenerating tail tip after treatment with 1 μM MPA and 200 μM guanosine (R).

(S) Quantification of IMPDH2 superstructures per 2500 μm^2 in either the non-regenerating trunk tissue or the regenerating tail tip treated with either 0.05% DMSO, 1 μM MPA, 10 μM MPA, or 25 μM MPA.

(T) Quantification of IMPDH2 superstructures per 2500 μm^2 in tadpole tail tips treated with 1uM MPA vs 1 μM MPA + 200 μM guanosine. Statistical significance was determined by Welch's t-test. **p<0.01.

Discussion

Our results suggest that IMPDH function is essential for efficient tail regeneration in *X. tropicalis*. Regeneration engages a number of cellular processes which require abundant purine nucleotides, and so a role for this enzyme would be expected to support those processes. Our data also show that IMPDH inhibition leads to significantly reduced cell proliferation, though these data do not discriminate between the many possible functions of a carefully regulated balance of ATP and GTP. We also find that IMPDH2 expression increases in regenerating tail tissues by 72 hpa, which coincides with the time at which cell proliferation increases during regeneration.[21,22] Among the most expensive cell functions for GTP during proliferation are DNA synthesis, protein synthesis, and spindle assembly, as each tubulin monomer requires GTP hydrolysis for microtubule assembly.[23] It seems likely that these functions would rely heavily on IMPDH to maintain sufficient levels of GTP relative to ATP. An intriguing focus for future analysis

is to identify the specific cellular functions that create the most dynamic demand for GTP, and which are the most sensitive to IMPDH inhibition.

This work also establishes that IMPDH2 is able to form filamentous superstructures in the *Xenopus* tail, and that these superstructures can form in multiple cell types without disrupting the overall morphology or behavior of the tadpole. This sets the stage for further examination of the role of enzyme filaments in vertebrate development. An intriguing observation is that superstructures were especially abundant in and followed the regular segmentation pattern of the somites. This raises questions about potential cell type-specific functions for IMPDH2 and filament assembly. Notably, other enzymes in the purine biosynthesis pathway, specifically adenylosuccinate lyase (ADSL), are required for muscle development in *Xenopus*.[24] Patient alleles of IMPDH2 that affect filament formation are associated with motor deficits, which may be attributable to changes in purinogenesis in either muscle cells, neurons, or both.[3] IMPDH2 function is also required for development of the enteric nervous system in mice.[25] As both muscle and neurons are cell types with high dynamic demand for ATP and GTP in cytoskeletal roles, these observations raise the possibility that IMPDH2 may play specific roles in the development or regeneration of these cell types. Experiments to interrogate the impact of filament-disrupting IMPDH2 variants on development and regeneration are now underway.

The propensity to form IMPDH2 filaments is not the same under all conditions. In the uninjured tail, we found that IMPDH2 filament superstructures form only when the enzyme is strongly inhibited. However, after injury, changes in IMPDH2 localization near the wound site occurred within 15 minutes, even in the absence of an inhibitor. These dynamics illustrate that IMPDH2 activity and localization can change rapidly in complex tissues. There are many cases where temporally or spatially localized conditions of purine stress may occur in the embryo, leading to specifically localized IMPDH2 filaments, that remain open to future investigation. For example, retinal IMPDH1 variants assemble into filamentous superstructures in photoreceptor cells, whose dynamics may be controlled by reversible phosphorylation.[26–28] The ability to form IMPDH2 filament structures is also crucial to the proliferation of ESCs in the developing mouse embryo, and occurs dynamically through embryogenesis.[29] These considerations highlight the importance of studying enzyme filaments or complexes in the context of whole tissues, not just in isolated cell types. We also note that the filament superstructures that we observe following IMPDH inhibition are large, micron-scale bundles of laterally associated filaments. The localized punctae we observed in the first few hours after injury were smaller, but still much larger than individual filaments. Our study leaves open the possibility that other dynamic assemblies of IMPDH2, including small individual filaments or multi-enzyme assemblies like purinosomes[30], may also form during regeneration and contribute to cell behavior.

Finally, we find that tail regeneration creates a sensitized condition in which a small added purine stress leads to filament assembly when it would not in uninjured tissue. It has not previously been known whether nucleotide demand is a physiologically important constraint in regeneration. The sensitization of regenerating tissue to filament formation suggests that the demand for purines, or GTP specifically, is higher in regenerating tissue than in similar non-regenerating tissue. This is consistent with purine biosynthesis being one potential target of the observed upregulation of the pentose phosphate pathway in regeneration[1], although others may well contribute, such as NADPH production for redox homeostasis or lipid biosynthesis, as

has also been suggested.[31,32] Overall, the propensity for IMPDH2 filament assembly represents a useful insight toward understanding how injured tissue mobilizes its metabolic resources toward wound healing and cell proliferation: if ATP and GTP are sunk into DNA or RNA biosynthesis, both of these purines would need to be replenished. IMPDH2 filament formation in the regenerating tissue would allow GTP to be rapidly produced in tandem with ATP, and would also allow GTP production to be favored under cell conditions where it is specifically needed in abundance.

Methods

Xenopus tropicalis husbandry and use

Use of *Xenopus tropicalis* was carried out under the approval and oversight of the IACUC committee at UW, an AALAC-accredited institution, under animal protocol 4374-01. Ovulation of adult *Xenopus tropicalis* and generation of embryos by natural matings were performed according to published methods.[33,34] Embryos were reared as described in Khokha et al.[33] Staging was assessed by the Nieuwkoop and Faber (NF) staging series.[35] Tadpoles were reared at 22 °C to stage 41 (3 dpf) and experiments were performed as described below. Animals were reared in petri dishes at a density of no more than 2 tadpoles/mL of rearing media, 1/9th Modified Ringer's solution (1/9x MR), and clutchmates were randomly assigned to treatment groups. Sex is not able to be determined by this stage and so is not a relevant biological variable. Tadpoles do not begin to feed independently until stage 45/46 and were not fed during the course of these experiments.

Xenopus tropicalis amputation assay

NF stage 41 tadpoles were anesthetized with 0.016% MS-222 in 1/9x MR and tested for response to touch prior to amputation surgery. Once fully anesthetized, a sterilized scalpel was used to amputate the posterior third of the tail. Amputated tadpoles were removed from anesthetic media within 10 minutes of amputation into 1/9x MR with or without added pharmacological inhibitors. Tadpoles were kept at a density of no more than 2.5 tadpoles per mL. For measurements of IMPDH2 inhibition and sensitized superstructure assembly, tadpoles were fixed at 72 hpa. For observation of early regeneration, tadpoles were fixed at 15 minutes, 1 hour, 6 hours, and 24 hours post amputation. Tadpoles were fixed in 1x MEM with 3.7% formaldehyde for 50 minutes at room temperature.

Pharmacological inhibition

Mycophenolic Acid (MPA) (MilliporeSigma M5255) was resuspended to a 200 mM stock in DMSO and Ribavirin (RBV) (Cayman Chemical 16757) to a 500 mM stock in DMSO. Guanosine (MilliporeSigma G6264) was resuspended directly in 1/9x MR to a concentration of 200 μM immediately prior to amputation. To verify IMPDH2 superstructure formation in tadpoles, uninjured and injured tadpoles were reared with 0.05% DMSO, 100 μM MPA, or 500 μM RBV diluted in 1/9x MR until collection at 72 hours following treatment. To induce a sensitized-regenerative condition, injured tadpoles were reared with 0.05% DMSO, 1 μM MPA, 10 μM MPA, 25 μM MPA, 200 μM Guanosine, or 1 μM MPA + 200 μM Guanosine diluted in 1/9x MR until collection at 72 hours following treatment. RBV was also used to characterize the sensitized-regenerative condition and is reported in **Supplementary Figure 2**.

Tail regeneration length analysis

Stereoscope imaging for regeneration length quantification was performed on a Leica M205 FA with a color camera. Fixed tadpoles were imaged in 1x PBS on 1% agarose pads and measurements were recorded using LAS X software. Representative images were acquired using a Leica DM 5500 B microscope using a 10x objective and processed using FIJI image analysis software.[36]

Immunohistochemistry

Fixed tadpoles were permeabilized by washing 3 × 20 minutes in 1x PBS + 0.01% Triton X-100 (PBS-Triton). Tadpoles were blocked for 1 hour at room temperature in 10% CAS-block (Invitrogen #00-8120) in PBS-Triton. Tadpoles were then incubated in primary antibody [1:100 rabbit anti-IMPDH2, proteintech 12948-1-AP; 1:1000 mouse anti-Histone H3 (phospho S10), Abcam ab14955] diluted in 100% CAS-block overnight at 4°C. Tadpoles were washed 3 × 10 minutes at room temperature in PBS-Triton then blocked for 30 minutes in 10% CAS-block in PBS-Triton. Secondary antibody (goat anti-rabbit 488, Invitrogen A11008; goat-anti mouse 594, Abcam ab150116) was diluted 1:500 in 100% CAS-block and incubated for 2 hours at room temperature. Tadpoles were then washed 3 × 10 minutes in PBS-Triton followed by a 10 minute incubation in 1:2000 DAPI (Sigma D9542) in PBS-Triton before 3 × 20 minute washes in PBS-Triton. Isolated tails were mounted on slides in ProLong Diamond (ThermoFisher P36970). Images were acquired using a Leica DM 5500 B microscope with 10X, 20X and 40X objectives and processed using Fiji image analysis software.

Cell proliferation assay

Images of pH3 stains were imported into Fiji. The amputation plane was identified, and the regenerating tissue area was measured. Then, the number of pH3 positive cells within the regenerating tissue was counted. Density of pH3 cells was determined by dividing the number of pH3 positive cells by the total area of regenerating tissue. Density was normalized to DMSO controls so that data from multiple clutches could be analyzed in tandem.

Whole-mount *in situ* hybridization

Tadpoles were fixed in 1x MEM with 3.7% formaldehyde for 45 minutes at room temperature. *Xenopus tropicalis* multibasket *in situ* hybridization protocols were followed as described by Khokha et al.[33], with pre-hybridization performed overnight. Whole tadpoles were imaged in 1x PBS + 0.1% Tween-20 on a bed of 1% agarose using a Leica M205 FA stereomicroscope with a color camera. Probes were synthesized using the following primer pair designed against a single exon of the *impdh2* transcript: forward - gcaagttgcccattgttaatggc, reverse - TAATACGACTCACTATAGGGaaggaccacggcatccac.

Western blotting

Tadpoles were anesthetized with 0.016% MS-222 in 1/9x MR and tested for response to touch prior to amputation surgery. For each experimental group, 10 tadpole tails were amputated just posterior to the vent and homogenized on ice in 100 µL of lysis buffer (50 mM Tris pH 7.6, 150 mM NaCl, 10 mM EDTA, 0.1% Triton X-100, Roche cOmplete™ Protease Inhibitor Cocktail).

Homogenized samples were centrifuged at 18,400xg for 20 minutes at 4°C. The soluble fraction was collected, and total protein concentration was quantified with a Pierce BCA assay (Thermo Scientific 23227). Samples were denatured by adding 1/4 volume of 4X Protein Sample Loading Buffer (Licor 928-40004). The total protein concentration of each sample was normalized according to the BCA assay by adding additional 1X Protein Sample Loading Buffer (4X Protein Sample Loading Buffer diluted to 1X with lysis buffer). Samples were heated at 100 °C for 5 minutes. Equal inputs of the samples were run on a 4-20% Mini-PROTEAN TGX precast gel (BIO-RAD 4561094) at 180 V for 40 minutes in manufacturer recommended running buffer (25 mM Tris, 192 mM glycine, 0.1% SDS, pH 8.3). Transfer to a nitrocellulose membrane was done using an Invitrogen Power Blotter Select Transfer Stack (Thermo Fisher PB3310) on an Invitrogen Power Blotter System (Thermo Fisher PB0012) using the Mixed Range MW Pre-Programmed method (constant 2.5 A with 25 V limit for 7 minutes). Membrane was incubated in Intercept PBS Blocking Buffer (Licor 927-70001) for 1 hour at 25°C with rocking. Membrane was added into 5 mL of 1X PBS-Tween (137 mM NaCl, 2.7 mM KCl, 10 mM Na2HPO4, 1.8 mM KH2PO4, 0.1% w/v Tween-20 detergent) and 5 mL of Intercept PBS Blocking Buffer. Membrane was incubated in primary antibodies: 1:1000 rabbit anti-IMPDH2 (Proteintech 12948-1-AP) and 1:3000 mouse anti-β-actin (Santa Cruz Biotech sc-47778) overnight, shaking at 4 °C. Membrane was washed with 1X PBS-Tween for 4x5min, then added into 5mL of 1X PBS-Tween mixed with 5mL of Intercept PBS Blocking Buffer. Membrane was incubated in the dark for 1 hour, shaking at 25 °C with secondary antibodies: 1:10000 goat anti-rabbit IgG (H+L) (DyLight 800 Fisher PISA510036) and 1:10000 goat anti-mouse IgG (H+L) (DyLight 680 Fisher PI35518). After 4 x 5 min washes in 1X PBS-Tween, the membrane was imaged on a LI-COR Imaging System (LI-COR Biosciences). Quantification of western blots was done in Fiji.

mRNA synthesis and injections

Plasmid pCS107_IMPDH2-RFP was synthesized using Gibson assembly following PCR amplification with the following primers: hIMPDH2 template (forward - GCTCGCCACCatggccgactacctgattagtg, reverse - GTACCGTCGAgaaaagccgcttctcatacgaa) and pCS107_Cterm-RFP (forward - gcggctttttcTCGACGGTACCGCGGGCCCG, reverse - tagtcggccatGGTGGCGAGCTCGAGATCCTG). Final construct was sequence verified before *in vitro* transcription. Plasmid DNA was linearized using *AscI* enzyme and mRNA was transcribed with SP6 mMessage mMachine kit (Invitrogen). mRNA was injected into embryos at the 2-cell stage at a dose of 1000 pg/embryo.

Live imaging

Tadpoles were anesthetized with 0.016% MS-222 in 1/9x MR and then mounted within 1% LMP agarose on coverslip-bottom dishes as described by Kieserman et al.[37] Immobilized tadpoles were imaged using a Leica SP8 confocal microscope with a 20x objective.

Analysis of previously published datasets

Published RNA-sequencing data (CPM and statistical analysis) was obtained from the NCBI Gene expression Omnibus (GEO) under accession number GSE174798.[19]

Quantification and statistical analysis

Boxplots were generated using the R package ggplot2.[38] Length and cell proliferation measurements were compared using ANOVA and post hoc Tukey's HSD test to identify differences between groups. For bulk RNA-seq analysis, statistically significant changes in gene expression were determined using edgeR.[39] Superstructure density in the regenerating tails of tadpoles treated with MPA with or without guanosine was compared using Welch's t-test. All statistical analyses were performed with R statistical software.[40] Information regarding statistics can be found in the figure legends.

Acknowledgements

This work was supported by a University of Washington Levinson fellowship to MEM, by a Helen Hay Whitney Foundation fellowship to SJC, and by grants R35GM149542 to JMK, R01GM148490 to AEW, and R01NS099124 to AEW. The authors gratefully acknowledge members of the Wills and Kollman labs for helpful discussion throughout the execution of this work.

Author contributions

Study conception and experimental design: MEM, GMW, AGO, JHP, JMK, AEW. Performing experiments: MEM, GMW, AGO, JHP, ZRL. Analyzing experiments: MEM, GMW, AGO, JHP, ZRL, AEW. Manuscript draft: MEM, GMW, AGO, AEW. Manuscript revision: MEM, GMW, AGO, JHP, ZRL, SJC, JMK, AEW. Funding: JMK, AEW.

References

1. Patel, J.H., Ong, D.J., Williams, C.R., Callies, L.K., and Wills, A.E. (2022). Elevated pentose phosphate pathway flux supports appendage regeneration. Cell Rep. *41*, 111552. https://doi.org/10.1016/j.celrep.2022.111552.
2. TeSlaa, T., Ralser, M., Fan, J., and Rabinowitz, J.D. (2023). The pentose phosphate pathway in health and disease. Nat. Metab. *5*, 1275–1289. https://doi.org/10.1038/s42255-023-00863-2.
3. Burrell, A.L., and Kollman, J.M. (2022). IMPDH dysregulation in disease: a mini review. Biochem. Soc. Trans. *50*, 71–82. https://doi.org/10.1042/BST20210446.
4. Johnson, M.C., and Kollman, J.M. (2020). Cryo-EM structures demonstrate human IMPDH2 filament assembly tunes allosteric regulation. eLife *9*, e53243. https://doi.org/10.7554/eLife.53243.
5. Thomas, E.C., Gunter, J.H., Webster, J.A., Schieber, N.L., Oorschot, V., Parton, R.G., and Whitehead, J.P. (2012). Different Characteristics and Nucleotide Binding Properties of Inosine Monophosphate Dehydrogenase (IMPDH) Isoforms. PLoS ONE *7*, e51096. https://doi.org/10.1371/journal.pone.0051096.
6. Juda, P., Šmigová, J., Kováčik, L., Bártová, E., and Raška, I. (2014). Ultrastructure of Cytoplasmic and Nuclear Inosine-5'-Monophosphate Dehydrogenase 2 "Rods and Rings" Inclusions. J. Histochem. Cytochem. *62*, 739–750. https://doi.org/10.1369/0022155414543853.
7. Ji, Y., Gu, J., Makhov, A.M., Griffith, J.D., and Mitchell, B.S. (2006). Regulation of the interaction of inosine monophosphate dehydrogenase with mycophenolic Acid by GTP. J. Biol. Chem. *281*, 206–212. https://doi.org/10.1074/jbc.M507056200.
8. Carcamo, W.C., Satoh, M., Kasahara, H., Terada, N., Hamazaki, T., Chan, J.Y.F., Yao, B., Tamayo, S., Covini, G., von Mühlen, C.A., et al. (2011). Induction of cytoplasmic rods and rings structures by inhibition of the CTP and GTP synthetic pathway in mammalian cells. PloS One *6*, e29690. https://doi.org/10.1371/journal.pone.0029690.
9. Calise, S.J., Carcamo, W.C., Krueger, C., Yin, J.D., Purich, D.L., and Chan, E.K.L. (2014). Glutamine deprivation initiates reversible assembly of mammalian rods and rings. Cell. Mol. Life Sci. CMLS *71*, 2963–2973. https://doi.org/10.1007/s00018-014-1567-6.
10. Jackson, R.C., Weber, G., and Morris, H.P. (1975). IMP dehydrogenase, an enzyme linked with proliferation and malignancy. Nature *256*, 331–333. https://doi.org/10.1038/256331a0.
11. Senda, M., and Natsumeda, Y. (1994). Tissue-differential expression of two distinct genes for human IMP dehydrogenase (E.C.1.1.1.205). Life Sci. *54*, 1917–1926. https://doi.org/10.1016/0024-3205(94)90150-3.
12. Collart, F.R., Chubb, C.B., Mirkin, B.L., and Huberman, E. (1992). Increased inosine-5'-phosphate dehydrogenase gene expression in solid tumor tissues and tumor cell lines. Cancer Res. *52*, 5826–5828. https://doi.org/10.2172/10148922.
13. Nagai, M., Natsumeda, Y., and Weber, G. (1992). Proliferation-linked regulation of type II IMP dehydrogenase gene in human normal lymphocytes and HL-60 leukemic cells. Cancer Res. *52*, 258–261.
14. Hedstrom, L. (1999). IMP dehydrogenase: mechanism of action and inhibition. Curr. Med. Chem. *6*, 545–560.
15. Sintchak, M.D., Fleming, M.A., Futer, O., Raybuck, S.A., Chambers, S.P., Caron, P.R., Murcko, M.A., and Wilson, K.P. (1996). Structure and mechanism of inosine monophosphate dehydrogenase in complex with the immunosuppressant mycophenolic acid. Cell *85*, 921–930. https://doi.org/10.1016/s0092-8674(00)81275-1.
16. Franklin, T.J., and Cook, J.M. (1969). The inhibition of nucleic acid synthesis by mycophenolic acid. Biochem. J. *113*, 515–524. https://doi.org/10.1042/bj1130515.
17. Hager, P.W., Collart, F.R., Huberman, E., and Mitchell, B.S. (1995). Recombinant human inosine monophosphate dehydrogenase type I and type II proteins: Purification and

characterization of inhibitor binding. Biochem. Pharmacol. *49*, 1323–1329. https://doi.org/10.1016/0006-2952(95)00026-V.

18. Streeter, D.G., Witkowski, J.T., Khare, G.P., Sidwell, R.W., Bauer, R.J., Robins, R.K., and Simon, L.N. (1973). Mechanism of action of 1- -D-ribofuranosyl-1,2,4-triazole-3-carboxamide (Virazole), a new broad-spectrum antiviral agent. Proc. Natl. Acad. Sci. U. S. A. *70*, 1174–1178. https://doi.org/10.1073/pnas.70.4.1174.
19. Patel, J.H., Schattinger, P.A., Takayoshi, E.E., and Wills, A.E. (2022). Hif1α and Wnt are required for posterior gene expression during Xenopus tropicalis tail regeneration. Dev. Biol. *483*, 157–168. https://doi.org/10.1016/j.ydbio.2022.01.007.
20. Wu, X., Zhong, H., Song, J., Damoiseaux, R., Yang, Z., and Lin, S. (2006). Mycophenolic Acid Is a Potent Inhibitor of Angiogenesis. Arterioscler. Thromb. Vasc. Biol. *26*, 2414–2416. https://doi.org/10.1161/01.ATV.0000238361.07225.fc.
21. Love, N.R., Chen, Y., Bonev, B., Gilchrist, M.J., Fairclough, L., Lea, R., Mohun, T.J., Paredes, R., Zeef, L.A.H., and Amaya, E. (2011). Genome-wide analysis of gene expression during Xenopus tropicalis tadpole tail regeneration. BMC Dev. Biol. *11*, 70. https://doi.org/10.1186/1471-213X-11-70.
22. Kakebeen, A.D., Chitsazan, A.D., Williams, M.C., Saunders, L.M., and Wills, A.E. (2020). Chromatin accessibility dynamics and single cell RNA-Seq reveal new regulators of regeneration in neural progenitors. eLife *9*, e52648. https://doi.org/10.7554/eLife.52648.
23. Barisic, M., Rajendraprasad, G., and Steblyanko, Y. (2021). The metaphase spindle at steady state - Mechanism and functions of microtubule poleward flux. Semin. Cell Dev. Biol. *117*, 99–117. https://doi.org/10.1016/j.semcdb.2021.05.016.
24. Duperray, M., Hardet, F., Henriet, E., Saint-Marc, C., Boué-Grabot, E., Daignan-Fornier, B., Massé, K., and Pinson, B. (2023). Purine Biosynthesis Pathways Are Required for Myogenesis in Xenopus laevis. Cells *12*, 2379. https://doi.org/10.3390/cells12192379.
25. Lake, J.I., Avetisyan, M., Zimmermann, A.G., and Heuckeroth, R.O. (2016). Neural crest requires Impdh2 for development of the enteric nervous system, great vessels, and craniofacial skeleton. Dev. Biol. *409*, 152–165. https://doi.org/10.1016/j.ydbio.2015.11.004.
26. Cleghorn, W.M., Burrell, A.L., Giarmarco, M.M., Brock, D.C., Wang, Y., Chambers, Z.S., Du, J., Kollman, J.M., and Brockerhoff, S.E. (2022). A highly conserved zebrafish IMPDH retinal isoform produces the majority of guanine and forms dynamic protein filaments in photoreceptor cells. J. Biol. Chem. *298*, 101441. https://doi.org/10.1016/j.jbc.2021.101441.
27. Plana-Bonamaisó, A., López-Begines, S., Fernández-Justel, D., Junza, A., Soler-Tapia, A., Andilla, J., Loza-Alvarez, P., Rosa, J.L., Miralles, E., Casals, I., et al. (2020). Post-translational regulation of retinal IMPDH1 in vivo to adjust GTP synthesis to illumination conditions. eLife *9*, e56418. https://doi.org/10.7554/eLife.56418.
28. Calise, S.J., O'Neill, A.G., Burrell, A.L., Dickinson, M.S., Molfino, J., Clarke, C., Quispe, J., Sokolov, D., Buey, R.M., and Kollman, J.M. (2024). Light-sensitive phosphorylation regulates retinal IMPDH1 activity and filament assembly. J. Cell Biol. *223*, e202310139. https://doi.org/10.1083/jcb.202310139.
29. Peng, M., Keppeke, G.D., Tsai, L.-K., Chang, C.-C., Liu, J.-L., and Sung, L.-Y. (2024). The IMPDH cytoophidium couples metabolism and fetal development in mice. Cell. Mol. Life Sci. CMLS *81*, 210. https://doi.org/10.1007/s00018-024-05233-z.
30. Zhao, H., Chiaro, C.R., Zhang, L., Smith, P.B., Chan, C.Y., Pedley, A.M., Pugh, R.J., French, J.B., Patterson, A.D., and Benkovic, S.J. (2015). Quantitative analysis of purine nucleotides indicates that purinosomes increase de novo purine biosynthesis. J. Biol. Chem. *290*, 6705–6713. https://doi.org/10.1074/jbc.M114.628701.
31. Love, N.R., Chen, Y., Ishibashi, S., Kritsiligkou, P., Lea, R., Koh, Y., Gallop, J.L., Dorey, K., and Amaya, E. (2013). Amputation-induced reactive oxygen species are required for successful Xenopus tadpole tail regeneration. Nat. Cell Biol. *15*, 222–228.

https://doi.org/10.1038/ncb2659.

32. Love, N.R., Ziegler, M., Chen, Y., and Amaya, E. (2014). Carbohydrate metabolism during vertebrate appendage regeneration: what is its role? How is it regulated?: A postulation that regenerating vertebrate appendages facilitate glycolytic and pentose phosphate pathways to fuel macromolecule biosynthesis. BioEssays News Rev. Mol. Cell. Dev. Biol. *36*, 27–33. https://doi.org/10.1002/bies.201300110.
33. Khokha, M.K., Chung, C., Bustamante, E.L., Gaw, L.W.K., Trott, K.A., Yeh, J., Lim, N., Lin, J.C.Y., Taverner, N., Amaya, E., et al. (2002). Techniques and probes for the study of Xenopus tropicalis development. Dev. Dyn. Off. Publ. Am. Assoc. Anat. *225*, 499–510. https://doi.org/10.1002/dvdy.10184.
34. Sive, H.L., Grainger, R.M., and Harland, R.M. (2000). Early Development of Xenopus Laevis: A Laboratory Manual (CSHL Press).
35. Nieuwkoop, P.D., and Fader, J. (1994). Normal table of Xenopus laevis (Daudin): a systematical and chronological survey of the development from the fertilized egg till the end of metamorphosis.
36. Schindelin, J., Arganda-Carreras, I., Frise, E., Kaynig, V., Longair, M., Pietzsch, T., Preibisch, S., Rueden, C., Saalfeld, S., Schmid, B., et al. (2012). Fiji: an open-source platform for biological-image analysis. Nat. Methods *9*, 676–682. https://doi.org/10.1038/nmeth.2019.
37. Kieserman, E.K., Lee, C., Gray, R.S., Park, T.J., and Wallingford, J.B. (2010). High-magnification in vivo imaging of Xenopus embryos for cell and developmental biology. Cold Spring Harb. Protoc. *2010*, pdb.prot5427. https://doi.org/10.1101/pdb.prot5427.
38. Wickham, H. (2009). ggplot2: Elegant Graphics for Data Analysis (Springer) https://doi.org/10.1007/978-0-387-98141-3.
39. Robinson, M.D., McCarthy, D.J., and Smyth, G.K. (2010). edgeR: a Bioconductor package for differential expression analysis of digital gene expression data. Bioinforma. Oxf. Engl. *26*, 139–140. https://doi.org/10.1093/bioinformatics/btp616.
40. R Core Team (2024). R: A Language and Environment for Statistical Computing. Version 4.4.1 (R Foundation for Statistical Computing). https://www.R-project.org.